

Subsynchronous Oscillations in Inverter-Dominated Power Systems

A.A. Suvorov^{1,*}, A.B. Askarov¹, V.E. Rudnik¹, I.N. Gusarov¹

¹ Tomsk Polytechnic University, Tomsk, Russia

Abstract— The number of electric power conversion devices connected to AC grids of different voltages has markedly increased worldwide in recent years due to the steady growth in renewable power capacity. Unique features of power inverters (high performance, the dominant role of the automatic control system, etc.) modify dynamic properties of power systems, resulting in new operating states and processes. These are, most notably, broadband oscillations and subsynchronous oscillations (SSO) in particular. The latter are the subject of the present study. One of the causes of such oscillations is interaction between automatic control systems running inverters and the external grid. A comprehensive SSO analysis within the study involved frequency analysis of simplified models of the grid-tie inverter under different patterns of active and reactive power control, as well as the detailed modeling in the time domain. The findings of the above analysis served as a basis for a taxonomy of SSO causation mechanisms, which are related to the dynamics of inverter's automatic control system operation under various network topologies and operating conditions. Furthermore, the factors increasing the probability of SSO events in power grids with inverter-based generators are highlighted. Testing different designs of closed-loop automatic control systems provided evidence for the validity of the proposed taxonomy.

Index Terms — Grid-tie inverter, subsynchronous oscillations, automatic control systems.

I. INTRODUCTION

The increased focus on environmental protection issues over the last decade and the corresponding policies pursued by countries worldwide to serve the steadily growing electricity demand facilitate a paradigm shift of the energy sector from conventional synchronous generators running on fossil fuels in favor of generation facilities based on renewable energy sources (RES) [1]. The transition from conventional generation to renewables is inextricably linked to the adoption of power inverters in modern power systems: at present, their use in power generation, transmission, distribution, and consumption is ever growing.

II. LITERATURE REVIEW

It has been demonstrated that grid-tie inverters connecting RES to AC grids and commonly operating in the grid-following mode fail to ensure stable operation in weak and ultraweak grids [2–5], when the short circuit ratio (SCR) at the point of inverter connection to the grid is less than 2. Furthermore, instability in such cases may be accompanied by broadband oscillations, most notably subsynchronous oscillations (SSO) [6] that are the subject of this study.

One of the causes of such oscillations is interaction between automatic control systems of inverters and an external grid, which over the last 15 years was responsible for SSO events ranging from a few Hz up to a few tens of Hz in power systems worldwide [7, 8]. In view of this, a primary challenge for the global energy sector is to investigate SSO induced by inverter control algorithms and characterize their causation mechanisms. The scope of this study covers some of the key findings of a comprehensive

* Corresponding author.
E-mail: suvorovaa@tpu.ru

DOI: [10.25729/esr.2026.01.0008](https://doi.org/10.25729/esr.2026.01.0008)

Received December 1, 2025. Revised January 15, 2026.
Accepted February 13, 2026. Available online March 31, 2026.

This is an open-access article under a Creative Commons Attribution-NonCommercial 4.0 International License.

© 2026 ESI SB RAS and authors. All rights reserved.

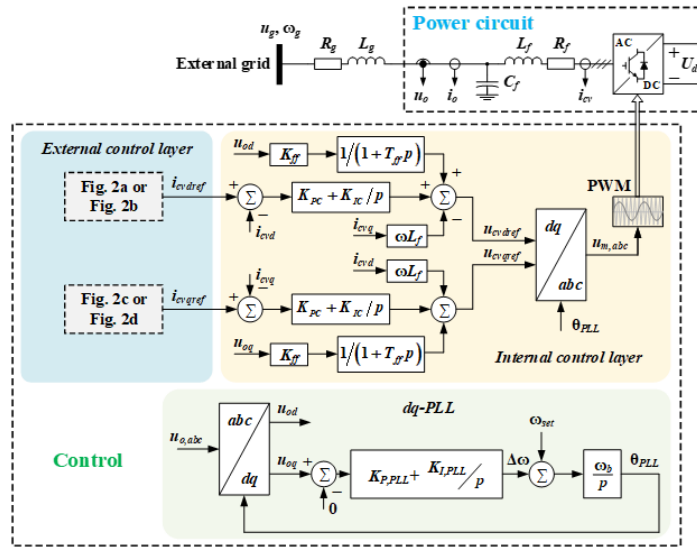


Fig. 1. The overall block diagram of the investigated electrical network with a grid-tie inverter.

analysis of SSO origins in power systems with high inverter penetration. More detailed treatment of the subject matter is available in our previous publications [9, 10].

III. METHODOLOGY

Figure 1 shows the block diagram of the investigated electrical network with a connected generic energy source, such as a PV system. Connecting the source to an external AC grid is implemented with a grid-tie inverter operating in the grid-following mode [11, 12]. Figure 2 presents a more detailed structure of possible options for external control loops of the grid-tie inverter.

Figure 1 shows that the three-phase inverter has decoupled control of active and reactive power in *dq*-axes rotating at the synchronous speed, where the *d*-axis coincides with the voltage vector at the point of connection. Inverter synchronization with the AC grid is achieved

through a phase-locked loop (PLL). This study covers the four most common scenarios of the grid-tie inverter control to facilitate further analysis:

- 1) P-U control: inverter's output active power is controlled along the direct axis *d*, whereas the voltage at the point of inverter's connection to the grid is controlled along the quadrature axis *q* (Figs. 2a and 2b);
- 2) P-Q control: inverter's output active and reactive powers are controlled along the direct and quadrature axes, respectively (Fig. 2a and 2d);
- 3) DVC-U control: inverter's output active power is controlled by DC voltage regulation along the direct axis, whereas voltage at the point of inverter's connection to the grid is controlled along the quadrature axis (Figs. 2b and 2c);
- 4) DVC-Q control: inverter's output active power is controlled by DC voltage regulation along the direct axis,

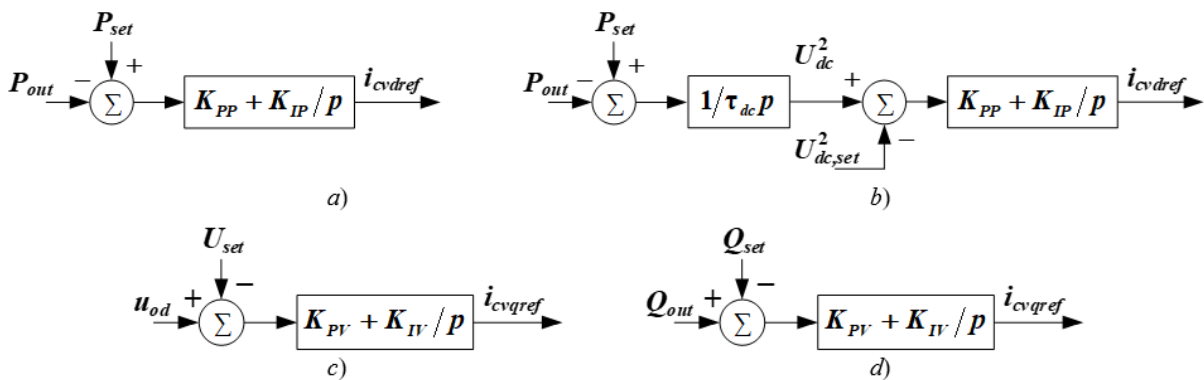


Fig. 2. Block diagrams of external control loops: a) – P control; b) – DVC control; c) – U control; d) – Q control.

whereas inverter's output reactive power is controlled along the quadrature axis (Figs. 2b and 2d).

To identify the causation mechanism of oscillations and the causes themselves, we establish simplified relationships that explicitly capture the interplay between different controllers, as well as effect of the topology and operating conditions of an electrical network. To this end, it is acceptable to represent a grid-tie inverter driven by a conventional control algorithm as current sources.

By way of an example, Fig. 3 shows the block diagram of a simplified model of a grid-tie inverter with active power regulation and PLL, where Block I corresponds to the active power regulator $G_{PC}^{cl}(p)$, Block II captures the effect of the PLL, and Block III is related to the voltage regulator $G_{VC}^{cl}(p)$.

Our analysis of the resulting expressions leverages the root locus method [13] that evaluates the stability of a closed-loop transfer function by the value of the gain coefficient at the point of intersection of locus branches with the imaginary axis. If this coefficient is less than 1, the closed system is deemed unstable in terms of the

considered equilibrium point.

Figure 4 uses three different colors to indicate zeros and poles corresponding to each of the above blocks, given the PLL broadband ($b_{w_{PLL}}$) of 13 Hz. Note that Block III poles move toward zeros z_2 and z_4 , Block II poles move toward z_1 and $-\infty$, and those of Block I – toward the origin (z_3) and $+\infty$, respectively. As a result, Block I poles, i.e. those of the voltage regulation loop (Fig. 2c), explicitly intersect the imaginary axis and pass through the right half-plane which affects the generation of oscillations in the considered case. The oscillations are thus caused by the use of the voltage regulation loop, which is responsible for interplay between active power and voltage control of the grid-tie inverter.

If the voltage control loop is replaced with the active power control loop, the coupled poles of Block I intersect the imaginary axis only at the origin, which eliminates oscillatory instability (red curves in Fig. 4). The factors that increase the likelihood of oscillation events are as follows: the grid impedance magnitude, the inverter's active power loading, and the voltage at the point of common coupling. Similarly, other combinations of

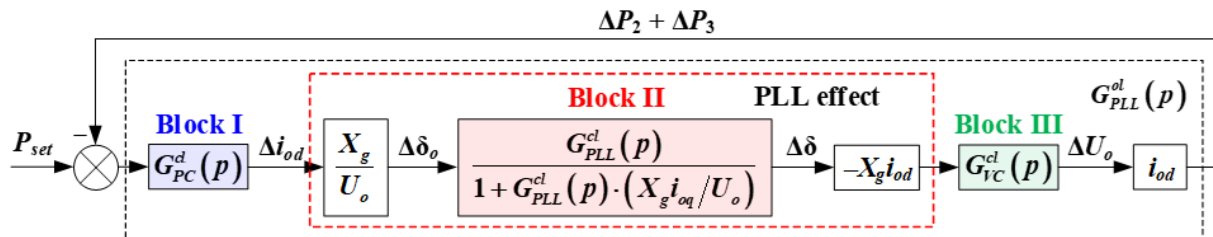


Fig. 3. The block diagram of a closed-loop transfer function that captures the effect of the PLL block on generation of oscillations.

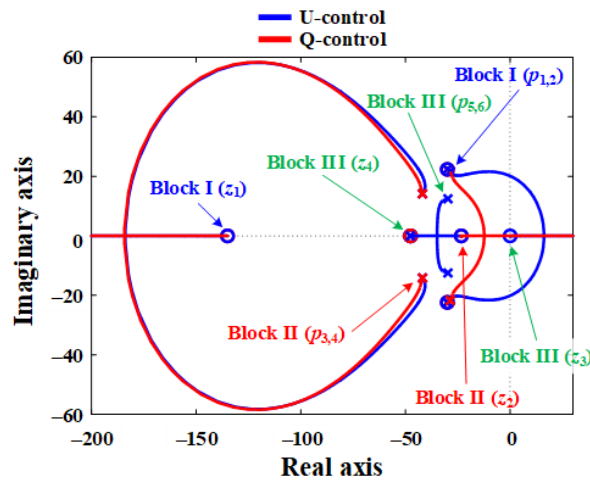


Fig. 4. Root locus plots for the open-loop function $G_{PLL}^{ol}(p)$, given the PLL bandwidth of 13 Hz and different regulators along the q-axis.

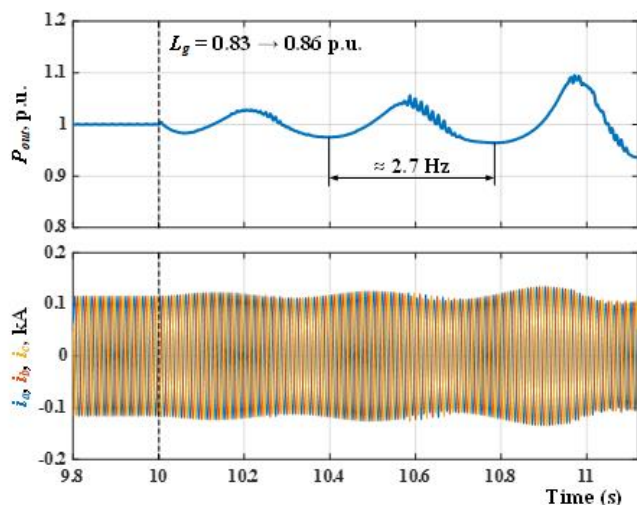


Fig. 5. Waveforms of processes in time domain modeling, given an L_g increase for P-U control with the PLL bandwidth of 13 Hz.

control algorithms of the grid-tie inverter are analyzed, as shown in Fig. 2.

IV. RESULTS

The findings of the analysis of linearized models of the grid-tie inverter controlled by different methods were validated by time domain simulations of the investigated system (Figs. 1 and 2) in the PSCAD (Power systems CAD) environment. Figure 5 shows the waveforms of the output active power and three-phase current of the inverter for the case of P-U control when the equivalent grid impedance changes.

It follows from Fig. 5, that the analysis of the detailed three-phase model of the inverter with P-U control reveals instability in the grid-tie inverter operation once the grid

impedance reaches a specific threshold ($L_g = 0.86$ p.u.). The instability is oscillatory in nature, with the dominant frequency of about 2.7 Hz. The frequency content of these oscillations was identified by analyzing the three-phase current frequency range applying the Fourier transform (Fig. 6). The highlighted frequency of 2.7 Hz is observed in the dq frame and is also characteristic of the inverter's active power oscillations. Furthermore, the frequency content analysis of the phase A current (Fig. 6) under P-U control, as performed in the fixed frame of reference, revealed the dominant frequencies of 47.2 Hz and 52.8 Hz. These values mirror each other with respect to fundamental grid frequency (50 Hz), corresponding to the oscillations frequency identified in the rotating frame of reference: $50 \pm 2.7 \approx 47.3$ and 52.7 Hz. This mirrored frequency

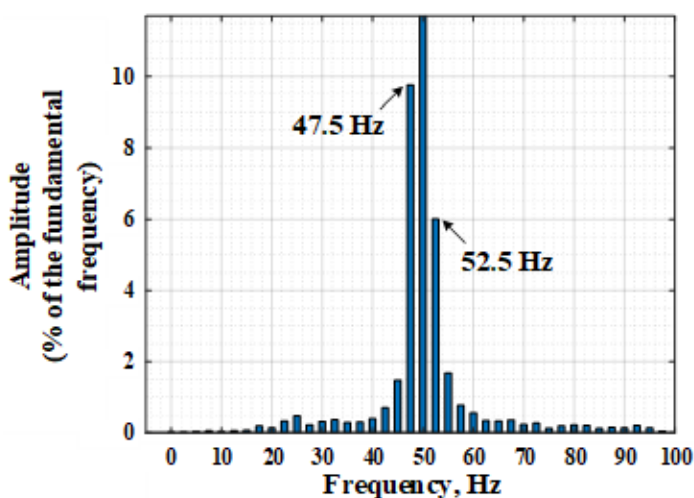


Fig. 6. The harmonic content of the phase A current after the onset of oscillations for the case of P-U control with the PLL bandwidth of 13 Hz.

arrangement confirms that the generated oscillations were caused by the inverter's control system operating in the rotating dq -axes [14].

Next, the experimental studies were performed by testing the closed-loop control system of a grid-tie inverter with the aid of the Real Time Digital Simulator (RTDS) [15] (Fig. 7). Control algorithms that use different regulation techniques were implemented in an STM32 industrial microcontroller that ensured a real-time control of the inverter's digital model in the RTDS environment. Figure 8 presents validation results for one of the operating conditions presented in Fig. 5. In this case, instability occurred when the grid impedance L_g increased to 0.85 p.u., which aligned with simulation results. The experiment also demonstrated that the increase in the response speed of the voltage regulator in the external control loop suppressed oscillations of about 2.7 Hz and growing amplitude, thus ensuring stable operation of the grid-tie inverter even in ultraweak grids.

V. DISCUSSION

Table 1 summarizes our findings on key oscillation causation mechanisms and their defining features.

A key risk factor triggering SSO events in grids with inverters are weak grid conditions that increase the equivalent grid impedance. The effect of active power loads on the dynamics of inverter's operation is inconsistent. Under most scenarios (not covered in this study), increasing the output active power of the inverter makes oscillation events more probable. However, when the performance of external regulators (e.g., active or reactive power regulators) is comparable to the dynamics of the PLL block, the inverse relationship may emerge. In such cases, the SSO events are more likely to occur as the inverter's output active power decreases. Another factor that has a direct effect on the emergence of oscillations is the PLL block dynamics. The frequency of the resulting oscillations is primarily determined by the bandwidth of the block as part of the inverter control system.

The analysis of the generated SSO revealed their two defining features. The first is a wide frequency spectrum, ranging from a few Hz to values approaching fundamental frequency of the grid, as evidenced by the experimental data in Table 1. The second is the presence of mirror frequencies located symmetrically relative to the fundamental frequency, as revealed by the analysis of

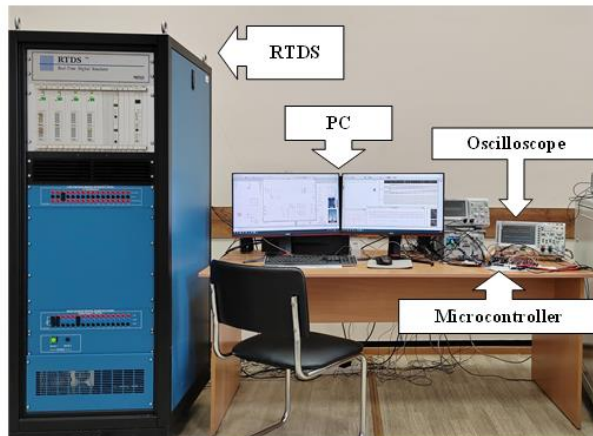


Fig. 7. The test rig for closed-loop testing.

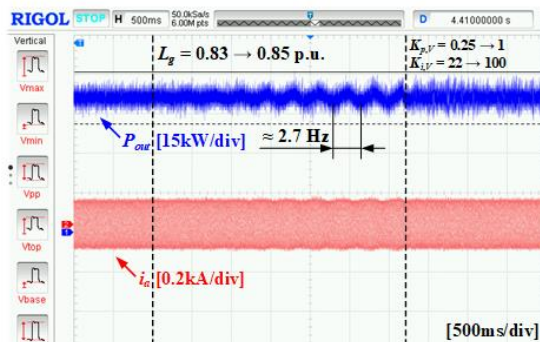


Fig. 8. Simulation results of closed-loop testing for the case of P-U control of the inverter, given the PLL bandwidth of 13 Hz

three-phase currents and voltages in the grid. This mirroring of the oscillation frequency content was observed in all the investigated scenarios and is an inherent result of the inverter's control system operation within the rotating dq reference frame. This feature may serve as a key criterion to distinguish SSO events specifically caused by the interaction of the grid-tie inverter control system with the parameters of an external grid under certain topological and operating conditions.

VI. CONCLUSIONS

This study presented the findings of an analysis of simplified control system models for grid-tie inverters with different external regulation loops that are commonly employed in conventional RES inverter control algorithms. The investigated models enabled the identification of specific loops that trigger SSO events in the grid, while determining the factors that increase their occurrence likelihood. By combining the frequency analysis of linearized models, mathematical modeling of the time domain, and closed-loop testing, this study developed a taxonomy of SSO causation mechanisms driven by the

dynamics of the grid-tie inverter control system under various topological and operating conditions. The presented taxonomy is based on the choice of regulators, whose combination determines the causation mechanism of oscillations. Network topology and operating conditions are also a major factor, which was duly reflected in the taxonomy design. These factors can trigger different causation mechanisms depending on their magnitude at the pre-fault state; in particular, this could be the level of active power loading. A distinct feature of the SSO type investigated in this study - the oscillations induced by the inverter control system – is a broad frequency range extending from low frequencies to the values close to the synchronous frequency, characterized by a mirrored synchronous frequency, characterized by a mirrored frequency arrangement in the case of three-phase quantities.

ACKNOWLEDGMENT

The research was supported by the Russian Science Foundation Grant No. 24-29-00004.

TABLE 1. Taxonomy of SSO Causation Mechanisms Related to the Inverter Control System

Control type		P-U control				P-Q control		
		bw_{PLL}		bw_{VC}	bw_{PLL}			
Condition		High	Medium	Low	High	High	Medium	Low
	Risk factors of SSO generation	L_g	Increase ↑					
i_{od}		↑	↑	↑	↓	↑	↑	↑
U_o		Decrease ↓						
Instability type		Oscillatory	Oscillatory	Oscillatory	Oscillatory	Oscillatory/aperiodic	Aperiodic	Aperiodic
SSO mirror frequency		yes	yes	yes	yes	yes/no	no	no
SSO frequency in the dq frame, Hz		≈25.3	≈2.8	≈1.96	≈25.6	≈27/-	-	-
SSO cause		PLL delays	PLL and VR interaction	PLL settings	PLL and VR interaction	PLL delays / none (transmitted power limit)	none (transmitted power limit)	none (transmitted power limit)
Control type		DVC-U control				DVC-Q control		
		bw_{PLL}		bw_{VC}	bw_{PLL}			
Condition		High	Medium	Low	High	High	Medium	Low
Risk factors of SSO generation	L_g	Increase ↑						
	i_{od}	↑	↑	↑	↓	↑	↑	↑
	U_o	Decrease ↓						
Instability type		Oscillatory	Oscillatory	Oscillatory	Oscillatory	Oscillatory	Aperiodic	Oscillatory
SSO mirror frequency		yes	yes	yes	yes	yes	no	yes
SSO frequency in the dq frame, Hz		≈26	≈4	≈3	≈24	≈27	-	≈1.3
SSO cause		PLL delays	DCVR settings	PLL settings	PLL and VR interaction	PLL delays	DCVR settings	DCVR settings

PR – active power regulator; VR – voltage regulator; DCVR – DC circuit voltage regulator

ABBREVIATIONS AND DESIGNATIONS

Designation	Explanation
u_g, ω_g	grid voltage and angular frequency
R_g, L_g	grid active resistance and inductance
u_o, i_o	output voltage and current
R_f, L_f, C_f	filter active resistance, inductance and capacity
i_{CV}	output current of the inverter
i_{CVd}, i_{CVq}	output current of the inverter on the d -axis and q -axis
U_{DC}	direct current voltage
PWM	pulse width modulation
i_{CVdref}, i_{CVqref}	reference output current of the inverter on the d -axis and q -axis
u_{CVdref}, u_{CVqref}	reference output voltage of the inverter on the d -axis and q -axis
u_{od}, u_{oq}	output voltage on the d -axis and q -axis
K_{ff}	voltage feedforward coefficient
T_{ff}	voltage feedforward time constant
K_{PC}, K_{IC}	proportional and integral coefficients of inner current control loop
$u_{m,abc}$	modulated voltage in a three-phase coordinate system
θ_{PLL}	voltage angle of phase-locked loop
$u_{o,abc}$	output voltage in a three-phase coordinate system
$K_{P,PLL}, K_{I,PLL}$	proportional and integral coefficients of phase-locked loop
$\Delta\omega$	angular frequency deviation
ω_{set}	angular frequency setpoint
ω_b	base angular frequency
P_{out}	output active power
P_{set}	active power setpoint
K_{PP}, K_{IP}	proportional and integral coefficients of active power control loop
τ_{dc}	direct current voltage control time constant
$U_{DC,set}$	direct current voltage setpoint
K_{PV}, K_{IV}	proportional and integral coefficients of voltage control loop
Q_{out}	output reactive power
Q_{set}	reactive power setpoint
$\Delta P_2, \Delta P_3$	active power deviation
G_{PC}^{cl}	closed-loop transfer function of active power control loop
i_{od}	output current on the d -axis
Δi_{od}	output current on the d -axis deviation
X_g	grid inductive resistance
$\Delta\delta_0$	power angle deviation
G_{PLL}^{cl}	closed-loop transfer function of phase-locked loop control
G_{VC}^{cl}	closed-loop transfer function of voltage control loop
G_{PLL}^{ol}	open-loop transfer function of phase-locked loop control
bw_{PLL}	phase-locked loop bandwidth
bw_{VC}	voltage control bandwidth

REFERENCES

- [1] D. N. Karamov, I. A. Mal'tsev, D. N. Ilyushin, K. V. Suslov, V. V. Skutel'nik, E. P. Emelyanov, "Review of the experience gained worldwide with incentivizing renewable energy development and the extent to which it is applicable to Russia," *Energetik*, no. 9, pp. 39–49, 2022. (In Russian)
- [2] A. B. Askarov, A. A. Suvorov, M. V. Andreyev, A. S. Gusev, "Revisiting modern principles of control of renewable energy sources based on the virtual synchronous generator," *PNRPU Bulletin. Electrical Engineering, Information Technology, Control Systems*, no. 41, pp. 5–30, 2022. (In Russian)
- [3] N. I. Voropai, "Directions and challenges of the transformation of electric power systems," *Elektrichestvo*, no. 7, pp. 12–21, 2020. (In Russian)
- [4] Y. Cheng, S. Huang, J. Rose, V.A. Pappu, J. Conto, "ERCOT subsynchronous resonance topology and frequency scan tool development," in *IEEE Power and Energy Society General Meeting*, Boston, MA, USA, pp. 1–5, 2016.
- [5] P. V. Ilyushin, A. V. Simonov, "Operation of inverter-based distributed energy sources as part of power systems and isolated power districts," *Relay protection and automation*, no. 2 (39), pp. 30–38, 2020. (In Russian)
- [6] T. G. Klimova, V. A. Revyakin, "Subsynchronous and supersynchronous oscillations generation and detection in power systems: a review," *Energetik*, no. 5, pp. 27–32, 2022. (In Russian)
- [7] Y. Cheng, et al, "Real-world subsynchronous oscillation events in power grids with high penetrations of inverter-based resources," *IEEE Transactions on Power Systems*, vol. 38, no. 1, pp. 316–330, 2023.
- [8] U. Perera, A. M. T. Oo, R. Zamora, "Sub synchronous oscillations under high penetration of renewables – a review of existing monitoring and damping methods, challenges, and research prospects," *Energies*, vol. 15, no. 22, Art. no. 8477, 2022.
- [9] A. A. Suvorov, "Causation mechanisms of subsynchronous oscillations in power systems with power inverters. Part 1," *Elektrichestvo*, no. 1, pp. 17–31, 2025. (In Russian)
- [10] A. A. Suvorov, "Causation mechanisms of subsynchronous oscillations in power systems with power inverters. Part 2," *Elektrichestvo*, no. 2, pp. 29–41, 2025. (In Russian)
- [11] S. F. Zarei, et al, "Control of grid-following inverters under unbalanced grid conditions," *IEEE Transactions on Energy Conversion*, vol. 35, no. 1, pp. 184–192, 2019.
- [12] W. Du, et al, "Modeling of grid-forming and grid-following inverters for dynamic simulation of large-scale distribution systems," *IEEE transactions on Power Delivery*, vol. 36, no. 4, pp. 2035–2045, 2020.
- [13] E. P. Popov, *The theory of linear systems of automatic regulation and control*, 2nd ed. Moscow, USSR: Nauka. The Main Editorial Office for Physical and Mathematical Literature, 1989, 304 p. (In Russian)
- [14] F. Salehi, et al, "Sub-synchronous control interaction detection: A real-time application," *IEEE Transactions on Power Delivery*, vol. 35, no. 1, pp. 106–116, 2020.

- [15] P. Forsyth, R. Kuffel, "Utility applications of a RTDS® Simulator," in *2007 International Power Engineering Conference (IPEC 2007)*, Singapore, 2007, pp. 112–117.



Aleksey A. Suvorov, Ph.D. in Engineering, is currently an Associate Professor in the Division for Power and Electrical Engineering of the School of Energy and Power Engineering at Tomsk Polytechnic University, Tomsk, Russia. His research interests include the modeling of renewable energy sources and energy storage systems, as well as the operation of power inverters and their impact on power quality and transient stability in modern power systems.



Alisher B. Askarov, Ph.D. in Engineering, is currently an Associate Professor in the Division for Power and Electrical Engineering of the School of Energy and Power Engineering at Tomsk Polytechnic University, Tomsk, Russia. His research interests include the integration of renewable energy sources into power grids using advanced power inverters, the modeling of battery energy storage systems, and the development of control algorithms to improve grid stability and power quality.



Vladimir Ye. Rudnik, Ph.D. in Engineering, is currently an Associate Professor in the Division for Power and Electrical Engineering of the School of Energy and Power Engineering at Tomsk Polytechnic University, Tomsk, Russia. His research interests include the development of control and protection systems for power grids with inverter-based renewable sources and energy storage, alongside the mathematical modeling of automatic control systems to ensure stable operation during transient processes.



Ivan N. Gusarov is a postgraduate student in the Division for Power and Electrical Engineering of the School of Energy and Power Engineering at Tomsk Polytechnic University, Tomsk, Russia. His research interests include the optimization of industrial power supply systems integrating renewable generation and battery storage, load modeling, demand-side management, and the mitigation of power quality issues stemming from intermittent renewable sources and inverter operation.